

Indirect unitarity violation entangled with matter effects in reactor antineutrino oscillations

Yu-Feng Li^{a*}, Zhi-zhong Xing^{a,b†}, Jing-yu Zhu^{a‡}

^aInstitute of High Energy Physics, and School of Physical Sciences,
University of Chinese Academy of Sciences, Beijing 100049, China

^bCenter for High Energy Physics, Peking University, Beijing 100080, China

Abstract

If finite but tiny masses of the three active neutrinos are generated via the canonical seesaw mechanism with three heavy sterile neutrinos, the 3×3 Pontecorvo-Maki-Nakagawa-Sakata neutrino mixing matrix V will not be exactly unitary. This kind of indirect unitarity violation can be probed in a precision reactor antineutrino oscillation experiment, but it may be entangled with terrestrial matter effects as both of them are very small. We calculate the probability of $\bar{\nu}_e \rightarrow \bar{\nu}_e$ oscillations in a good analytical approximation, and find that, besides the zero-distance effect, the effect of unitarity violation is always smaller than matter effects, and their entanglement does not appear until the next-to-leading-order oscillating terms are taken into account. Given a 20-kiloton JUNO-like liquid scintillator detector, we reaffirm that terrestrial matter effects should not be neglected but indirect unitarity violation makes no difference, and demonstrate that the experimental sensitivities to the neutrino mass ordering and a precision measurement of θ_{12} and $\Delta_{21} \equiv m_2^2 - m_1^2$ are robust.

PACS number(s): 14.60.Pq, 14.60.St, 13.15.+g.

*Email: liyufeng@ihep.ac.cn

†Email: xingzz@ihep.ac.cn

‡Email: zhujingyu@ihep.ac.cn

1 Introduction

Experimental neutrino physics is entering the era of precision measurements, in which some fundamental questions about the properties of massive neutrinos will hopefully be answered. One of the burning issues is whether there exist some extra (sterile) neutrino species which do not directly participate in the standard weak interactions. Such hypothetical neutrinos are well motivated in the canonical (type-I) seesaw mechanism [1, 2, 3, 4, 5, 6, 7], which works at a high energy scale far above the electroweak symmetry breaking scale — it can naturally generate finite but tiny Majorana masses for the standard-model neutrinos (i.e., the mass eigenstates ν_1 , ν_2 and ν_3 corresponding to the flavor eigenstates ν_e , ν_μ and ν_τ) and interpret the observed matter-antimatter asymmetry of the Universe via the canonical leptogenesis mechanism [8]¹. Assuming the existence of three heavy sterile neutrinos in this seesaw picture, one may write out the standard weak charged-current interactions in terms of the mass eigenstates of three charged leptons and six neutrinos as follows:

$$-\mathcal{L}_{\text{cc}} = \frac{g}{\sqrt{2}} \overline{\begin{pmatrix} e & \mu & \tau \end{pmatrix}_L} \gamma^\mu \left[V \begin{pmatrix} \nu_1 \\ \nu_2 \\ \nu_3 \end{pmatrix}_L + R \begin{pmatrix} \nu_4 \\ \nu_5 \\ \nu_6 \end{pmatrix}_L \right] W_\mu^- + \text{H.c.}, \quad (1)$$

where ν_4 , ν_5 and ν_6 stand for the three heavy-neutrino mass eigenstates, V is the 3×3 Pontecorvo-Maki-Nakagawa-Sakata (PMNS) flavor mixing matrix [14, 15], and R is a 3×3 matrix describing the strength of flavor mixing between (e, μ, τ) and (ν_4, ν_5, ν_6) . Because $VV^\dagger = \mathbf{1} - RR^\dagger$ holds [16], where $\mathbf{1}$ denotes the identity matrix, the PMNS matrix V is not exactly unitary. Following the full angle-phase parametrization of the whole 6×6 neutrino mixing matrix advocated in Refs. [17, 18] and taking account of the fact that all the mixing angles appearing in R must be very small, it is convenient to express V as $V = (\mathbf{1} - \kappa)U$, in which

$$U = \begin{pmatrix} U_{e1} & U_{e2} & U_{e3} \\ U_{\mu 1} & U_{\mu 2} & U_{\mu 3} \\ U_{\tau 1} & U_{\tau 2} & U_{\tau 3} \end{pmatrix} = \begin{pmatrix} c_{12}c_{13} & s_{12}c_{13} & \hat{s}_{13}^* \\ -s_{12}c_{23} - c_{12}\hat{s}_{13}s_{23} & c_{12}c_{23} - s_{12}\hat{s}_{13}s_{23} & c_{13}s_{23} \\ s_{12}s_{23} - c_{12}\hat{s}_{13}c_{23} & -c_{12}s_{23} - s_{12}\hat{s}_{13}c_{23} & c_{13}c_{23} \end{pmatrix}, \quad (2)$$

$$\kappa \simeq \frac{1}{2} \begin{pmatrix} \kappa_{11} & 0 & 0 \\ 0 & \kappa_{22} & 0 \\ 0 & 0 & \kappa_{33} \end{pmatrix} + \begin{pmatrix} 0 & 0 & 0 \\ \kappa_{21} & 0 & 0 \\ \kappa_{31} & \kappa_{32} & 0 \end{pmatrix}$$

with $\kappa_{ij} = \hat{s}_{i4}^* \hat{s}_{j4} + \hat{s}_{i5}^* \hat{s}_{j5} + \hat{s}_{i6}^* \hat{s}_{j6}$ for $i \geq j = 1, 2, 3$. Here the notations $c_{ij} \equiv \cos \theta_{ij}$, $s_{ij} \equiv \sin \theta_{ij}$ and $\hat{s}_{ij} \equiv s_{ij} e^{i\delta_{ij}}$ have been used, where θ_{ij} and δ_{ij} are the rotation and phase angles, respectively. It is obvious that nonzero κ_{ij} arise from the small mixing between light and heavy neutrino states described by θ_{ij} (for $i = 1, 2, 3$ and $j = 4, 5, 6$), and therefore they measure the deviation of V from U — the effect of *indirect* unitarity violation (UV) caused by the heavy degrees of freedom which do not directly take part in the low-energy lepton-flavor-violating processes, such as neutrino oscillations. The current limits on the *indirect* UV effect can be found in Refs. [19, 20, 21, 22],

¹Throughout this work we only focus on the seesaw-induced heavy sterile neutrinos. Light sterile neutrinos have also attracted a lot of phenomenological attention, but in general they are less motivated from a theoretical point of view, although they have been introduced so as to explain some ambiguous “anomalies” [9, 10, 11, 12, 13].

where the elements of $|VV^\dagger| = |(1 - \kappa)(1 - \kappa^\dagger)|$ are constrained from the electroweak precision observables, low energy weak measurements and the neutrino oscillation data. A typical and conservative expectation is that the magnitude of κ_{ij} should be smaller than 0.05, which indicates that the active-sterile mixing angles θ_{ij} (for $i = 1, 2, 3$ and $j = 4, 5, 6$) can be taken as large as 7.5° . So far a lot of attention has been paid to possible effects of indirect UV in the accelerator-based long-baseline neutrino oscillation experiments [19, 23, 24, 25, 26, 27, 28, 29, 30], and limited attention has also been given to this kind of effect in a reactor-based antineutrino oscillation experiment [31, 32, 33]. It is already known that the UV-induced “zero-distance effect” must appear in the “disappearance” oscillation probability $P(\bar{\nu}_\alpha \rightarrow \bar{\nu}_\alpha)$ (for $\alpha = e, \mu, \tau$) [31, 34], for example,

$$P(\bar{\nu}_e \rightarrow \bar{\nu}_e)|_{L=0} = c_{14}^4 c_{15}^4 c_{16}^4 \simeq 1 - 2\kappa_{11}, \quad (3)$$

but extracting this small effect is extremely difficult even though there is a near detector, because uncertainties associated with the reactor antineutrino flux are expected to be overwhelming considering the reactor antineutrino anomaly and spectral features for the reactor antineutrino fluxes at around 5 MeV. In this case one may wonder whether the oscillating terms of $P(\bar{\nu}_e \rightarrow \bar{\nu}_e)$ can provide some information about the indirect UV or not ².

As pointed out in Refs. [36, 37, 38], terrestrial matter effects should not be neglected in the JUNO-like reactor antineutrino oscillation experiment with the baseline length $L \simeq 53$ km [35], since their strength is essentially comparable with the experimental sensitivity to the neutrino mass ordering. Two natural and meaningful questions turn out to be: (a) how the indirect UV effect is entangled with matter effects in $\bar{\nu}_e \rightarrow \bar{\nu}_e$ oscillations; (b) whether they can be distinguished from each other. The main purpose of the present work is just to answer these two questions.

The remaining parts of this paper are organized as follows. In section 2 we derive the analytical expression of $P(\bar{\nu}_e \rightarrow \bar{\nu}_e)$ by including both indirect UV and terrestrial matter effects and making a good approximation for the antineutrino beam energy of a few MeV [39, 40]. Section 3 is devoted to some numerical simulations based on the setup of a JUNO-like detector in order to answer the above two questions. We find that the indirect UV effect is always smaller than terrestrial matter effects, and their entanglement does not appear until the next-to-leading-order oscillating terms are taken into account. We summarize our main results in section 4 with two concluding remarks: (a) indirect UV makes no difference in the JUNO-like experiment; (b) such an experiment’s sensitivities to the neutrino mass ordering and a precision measurement of θ_{12} and $\Delta_{21} \equiv m_2^2 - m_1^2$ are robust.

2 Analytical approximations of $P(\bar{\nu}_e \rightarrow \bar{\nu}_e)$

Of course, the three heavy sterile neutrinos are kinematically forbidden to take part in neutrino oscillations in any realistic accelerator- or reactor-based experiments. Given the indirect UV

²In the subsequent analytical calculations and numerical simulations we shall only focus the UV effect in the oscillating terms, and neglect the UV-induced zero-distance effect. The latter has been discussed, for example, in Ref. [31] and Chapter 3 of Ref. [35].

effect hidden in the PMNS matrix V , the effective Hamiltonian describing the propagation of the *antineutrino mass eigenstates* in matter with a constant density profile can be written as

$$\tilde{\mathcal{H}} = \begin{pmatrix} E_1 & 0 & 0 \\ 0 & E_2 & 0 \\ 0 & 0 & E_3 \end{pmatrix} - \frac{G_F}{\sqrt{2}} V^T \begin{pmatrix} 2N_e - N_n & 0 & 0 \\ 0 & -N_n & 0 \\ 0 & 0 & -N_n \end{pmatrix} V^*, \quad (4)$$

where $E_i \simeq E + m_i^2/(2E)$ with E and m_i being the beam energy and masses of antineutrinos respectively (for $i = 1, 2, 3$), G_F denotes the Fermi constant, N_e and N_n stand respectively for the electron and neutron densities in matter. It is clear that the neutral-current-induced coherent forward scattering effect (described by N_n) becomes trivial and negligible, if V is exactly unitary. Now this effect, together with the charged-current-induced coherent forward scattering effect (described by N_e and only sensitive to the e -flavored neutrinos and antineutrinos), constitutes the terrestrial matter effect and can thus modify the behavior of antineutrino oscillations. Note that in Eq. (4) and throughout this paper we denote all the quantities in matter with tilde hats as their counterparts of the corresponding vacuum quantities in the indirect UV framework.

We begin with the useful formula of the matter-modified antineutrino oscillation probability $\tilde{P}(\bar{\nu}_e \rightarrow \bar{\nu}_e)$ derived by Kimura, Takamura and Yokomura (KTY) [41, 42] and take account of the indirect UV effect [43]:

$$\tilde{P}(\bar{\nu}_e \rightarrow \bar{\nu}_e) = \frac{1}{(VV^\dagger)_{ee}^2} \left[|(V^*V^T)_{ee}|^2 - 4 \sum_{j < k} \text{Re} \left(\tilde{X}_j^{ee} \tilde{X}_k^{ee*} \right) \sin^2 \left(\frac{\Delta \tilde{E}_{jk} L}{2} \right) \right], \quad (5)$$

where $\Delta \tilde{E}_{jk} \equiv \tilde{E}_j - \tilde{E}_k$, L denotes the baseline length and $\tilde{X}_j^{ee} \equiv (V^*W)_{ej} (VW^*)_{ej}$ (for $j, k = 1, 2, 3$) with \tilde{E}_i being the eigenvalues of $\tilde{\mathcal{H}}$ and W_{ij} being the unitary matrix which diagonalizes $\tilde{\mathcal{H}}$ (i.e., $W^\dagger \tilde{\mathcal{H}} W = \text{Diag}\{\tilde{E}_1, \tilde{E}_2, \tilde{E}_3\}$). To be explicit,

$$\tilde{X}_j^{ee} = \sum_{k=1}^3 N_{jk} Y_k^{ee}, \quad (6)$$

in which

$$N = \begin{pmatrix} \frac{\tilde{E}_2 \tilde{E}_3}{\Delta \tilde{E}_{21} \Delta \tilde{E}_{31}} & -\frac{\tilde{E}_2 + \tilde{E}_3}{\Delta \tilde{E}_{21} \Delta \tilde{E}_{31}} & \frac{1}{\Delta \tilde{E}_{21} \Delta \tilde{E}_{31}} \\ -\frac{\tilde{E}_1 \tilde{E}_3}{\Delta \tilde{E}_{21} \Delta \tilde{E}_{32}} & \frac{\tilde{E}_1 + \tilde{E}_3}{\Delta \tilde{E}_{21} \Delta \tilde{E}_{32}} & -\frac{1}{\Delta \tilde{E}_{21} \Delta \tilde{E}_{32}} \\ \frac{\tilde{E}_1 \tilde{E}_2}{\Delta \tilde{E}_{31} \Delta \tilde{E}_{32}} & -\frac{\tilde{E}_1 + \tilde{E}_2}{\Delta \tilde{E}_{31} \Delta \tilde{E}_{32}} & \frac{1}{\Delta \tilde{E}_{31} \Delta \tilde{E}_{32}} \end{pmatrix}, \quad (7)$$

and $Y_k^{ee} = (V^* \tilde{\mathcal{H}}^{k-1} V^T)^{ee}$. Since \tilde{X}_j^{ee} are real and $\Delta \tilde{E}_{ij} = \tilde{\Delta}_{ij}/2E$ with $\tilde{\Delta}_{ij} \equiv \tilde{m}_i^2 - \tilde{m}_j^2$, the expression of $\tilde{P}(\bar{\nu}_e \rightarrow \bar{\nu}_e)$ in Eq. (5) can be rewritten as:

$$\tilde{P}(\bar{\nu}_e \rightarrow \bar{\nu}_e) = 1 - 4\hat{X}_1^{ee} \hat{X}_2^{ee} \sin^2 \tilde{F}_{21} - 4\hat{X}_1^{ee} \hat{X}_3^{ee} \sin^2 \tilde{F}_{31} - 4\hat{X}_2^{ee} \hat{X}_3^{ee} \sin^2 \tilde{F}_{32}, \quad (8)$$

where $\hat{X}_i^{ee} \equiv \tilde{X}_i^{ee}/(VV^\dagger)_{ee}$ (for $i = 1, 2, 3$), and $\tilde{F}_{ij} = 1267 \times \tilde{\Delta}_{ij} L/E$ with $\tilde{\Delta}_{ij}$ being in unit of eV^2 , L being in unit of km and E being in unit of MeV (for $ij = 21, 31, 32$). It is easy to check

that $\widehat{X}_1^{ee} + \widehat{X}_2^{ee} + \widehat{X}_3^{ee} = 1$ holds. In the absence of both UV and matter effects, one is therefore left with $\widehat{X}_i^{ee} = |U_{ei}|^2$, depending only on θ_{12} and θ_{13} .

The above equations tell us that once the eigenvalues \widetilde{E}_i are figured out, it will be straightforward to obtain the explicit expression of $\widetilde{P}(\bar{\nu}_e \rightarrow \bar{\nu}_e)$. Since the antineutrino beam energy E is only around a few MeV, one may calculate the eigenvalues of $\widetilde{\mathcal{H}}$ by expanding them in terms of the small parameters

$$\alpha \equiv \frac{\Delta_{21}}{\Delta_{31}}, \quad \beta \equiv \frac{2\sqrt{2} G_F N_e E}{\Delta_{31}}, \quad \gamma = \frac{\sqrt{2} G_F N_n E}{\Delta_{31}} \quad (9)$$

with $\Delta_{ij} \equiv m_i^2 - m_j^2$ (for $ij = 21, 31, 32$) in vacuum and the small elements of κ . It is certainly a very good approximation to take $N_e \simeq N_n$ in reality, so $\beta \simeq 2\gamma = A/\Delta_{31}$ with $A \equiv 2\sqrt{2} G_F N_e E$ being a common matter parameter. Given $A \sim 1.52 \times 10^{-4} \text{ eV}^2 Y_e(\rho/\text{g/cm}^3)(E/\text{GeV}) \simeq 1.98 \times 10^{-4} \text{ eV}^2 (E/\text{GeV})$ for $\rho \simeq 2.6 \text{ g/cm}^3$ and $E \sim 4 \text{ MeV}$ in reactor antineutrino experiments, β and γ are actually much smaller than α in magnitude:

$$\begin{aligned} \alpha &\simeq 3.1 \times 10^{-2} \times \frac{\Delta_{21}}{7.5 \times 10^{-5} \text{ eV}^2} \times \frac{\pm 2.4 \times 10^{-3} \text{ eV}^2}{\Delta_{31}}, \\ \beta &\simeq 3.3 \times 10^{-4} \times \frac{E}{4 \text{ MeV}} \times \frac{\pm 2.4 \times 10^{-3} \text{ eV}^2}{\Delta_{31}}, \\ \gamma &\simeq 1.6 \times 10^{-4} \times \frac{E}{4 \text{ MeV}} \times \frac{\pm 2.4 \times 10^{-3} \text{ eV}^2}{\Delta_{31}}, \end{aligned} \quad (10)$$

in which the “ \pm ” signs of Δ_{31} stand for the normal mass ordering (NMO) and inverted mass ordering (IMO) of three neutrinos, respectively. It is clear that $\beta \sim \gamma \sim \mathcal{O}(\alpha^2)$ holds. As for the small UV parameters, we take $\kappa_{11} \sim \kappa_{22} \sim \kappa_{33} \sim \kappa_{21} \sim \kappa_{31} \sim \kappa_{32} \sim \mathcal{O}(\alpha)$ as a reasonable assumption [19]. Now the effective Hamiltonian in Eq. (4) can be expressed as

$$\widetilde{\mathcal{H}} = E_1 \mathbf{1} + \frac{\Delta_{31}}{2E} U^T \Omega U^*, \quad (11)$$

where Ω is a dimensionless matrix containing both UV and matter effects:

$$\Omega = U^* \begin{pmatrix} 0 & 0 & 0 \\ 0 & \alpha & 0 \\ 0 & 0 & 1 \end{pmatrix} U^T - (\mathbf{1} - \kappa)^T \begin{pmatrix} \beta - \gamma & 0 & 0 \\ 0 & -\gamma & 0 \\ 0 & 0 & -\gamma \end{pmatrix} (\mathbf{1} - \kappa)^* . \quad (12)$$

By making some analytical approximations, one may first calculate the eigenvalues of Ω and then figure out the eigenvalues of $\widetilde{\mathcal{H}}$. After a straightforward but tedious exercise, we arrive at the expressions of the eigenvalues λ_i of Ω in matter as follows:

$$\begin{aligned} \lambda_1 &\simeq -\beta |U_{e1}|^2 + \gamma + \frac{1}{2} \left(\xi_1 - \frac{\xi_3 + 2\beta^2 |U_{e1}|^2 |U_{e2}|^2}{\alpha} \right), \\ \lambda_2 &\simeq \alpha - \beta |U_{e2}|^2 + \gamma + \frac{1}{2} \left(\xi_1 + \frac{\xi_3 + 2\beta^2 |U_{e1}|^2 |U_{e2}|^2}{\alpha} \right), \\ \lambda_3 &\simeq 1 - \beta |U_{e3}|^2 + \gamma - \xi_2, \end{aligned} \quad (13)$$

where ξ_i (for $i = 1, 2, 3$) measure the effect of indirect UV:

$$\begin{aligned}
\xi_1 &= \beta\kappa_{11}(1 - |U_{e3}|^2) - \gamma [\kappa_{11}(1 - |U_{e3}|^2) + \kappa_{22}(1 - |U_{\mu3}|^2) + \kappa_{33}(1 - |U_{\tau3}|^2) \\
&\quad - 2\text{Re}(\kappa_{21}U_{e3}U_{\mu3}^* + \kappa_{31}U_{e3}U_{\tau3}^* + \kappa_{32}U_{\mu3}U_{\tau3}^*)] , \\
\xi_2 &= -\beta\kappa_{11}|U_{e3}|^2 + \gamma [\kappa_{11}|U_{e3}|^2 + \kappa_{22}|U_{\mu3}|^2 + \kappa_{33}|U_{\tau3}|^2 \\
&\quad + 2\text{Re}(\kappa_{21}U_{e3}U_{\mu3}^* + \kappa_{31}U_{e3}U_{\tau3}^* + \kappa_{32}U_{\mu3}U_{\tau3}^*)] , \\
\xi_3 &= \alpha\beta\kappa_{11}(|U_{e2}|^2 - |U_{e1}|^2) + \alpha\gamma \{ \kappa_{11}(|U_{e1}|^2 - |U_{e2}|^2) \\
&\quad + \kappa_{22}(|U_{\mu1}|^2 - |U_{\mu2}|^2) + \kappa_{33}(|U_{\tau1}|^2 - |U_{\tau2}|^2) \\
&\quad + 2\text{Re}(\kappa_{21}U_{e3}U_{\mu3}^* + \kappa_{31}U_{e3}U_{\tau3}^* + \kappa_{32}U_{\mu3}U_{\tau3}^*) \\
&\quad - 4\text{Re}[\kappa_{21}(U_{e3}U_{\tau2} - U_{e2}U_{\tau3})(U_{\mu3}^*U_{\tau2}^* - U_{\mu2}^*U_{\tau3}^*) \\
&\quad + \kappa_{31}(U_{e2}U_{\mu3} - U_{e3}U_{\mu2})(U_{\mu3}^*U_{\tau2}^* - U_{\mu2}^*U_{\tau3}^*) \\
&\quad + \kappa_{32}(U_{e3}U_{\mu2} - U_{e2}U_{\mu3})(U_{e3}^*U_{\tau2}^* - U_{e2}^*U_{\tau3}^*)] \} . \tag{14}
\end{aligned}$$

One can see that in ξ_i the six UV parameters κ_{ij} are all entangled with the two matter parameters β and γ , implying that switching off the terrestrial matter effects will automatically remove the indirect UV effect from λ_i . This important observation tells us that it will be much harder to probe indirect UV for a low-energy oscillation experiment, because the latter involves much smaller terrestrial matter effects. Note that ξ_3 is more suppressed in magnitude than ξ_1 and ξ_2 , but it cannot be ignored in the expressions of λ_1 and λ_2 since the combination ξ_3/α should be comparable with the ξ_1 term in Eq. (13). With the help of Eq. (13), the eigenvalues of $\tilde{\mathcal{H}}$ can be directly obtained from $\tilde{E}_i = E_1 + \lambda_i\Delta_{31}/(2E)$. The three effective neutrino mass-squared differences $\tilde{\Delta}_{ij}$ defined below Eq. (7) turn out to be

$$\begin{aligned}
\tilde{\Delta}_{21} &\simeq \Delta_{31} \left[\alpha + \beta(|U_{e1}|^2 - |U_{e2}|^2) + \frac{1}{\alpha}(\xi_3 + 2\beta^2|U_{e1}|^2|U_{e2}|^2) \right] , \\
\tilde{\Delta}_{31} &\simeq \Delta_{31} \left[1 + \beta(|U_{e1}|^2 - |U_{e3}|^2) - \frac{1}{2}(\xi_1 + 2\xi_2) + \frac{1}{2\alpha}(\xi_3 + 2\beta^2|U_{e1}|^2|U_{e2}|^2) \right] , \\
\tilde{\Delta}_{32} &\simeq \Delta_{31} \left[1 - \alpha + \beta(|U_{e2}|^2 - |U_{e3}|^2) - \frac{1}{2}(\xi_1 + 2\xi_2) - \frac{1}{2\alpha}(\xi_3 + 2\beta^2|U_{e1}|^2|U_{e2}|^2) \right] . \tag{15}
\end{aligned}$$

One can see that $\tilde{\Delta}_{21} = \tilde{\Delta}_{31} - \tilde{\Delta}_{32}$ holds to the accuracy of the approximations made above.

For simplicity, we are going to use $\tilde{\mathcal{H}}' = \tilde{\mathcal{H}} - E_1\mathbf{1}$ to calculate the probability of $\bar{\nu}_e \rightarrow \bar{\nu}_e$ oscillations in the following, since such a shift of $\tilde{\mathcal{H}}$ does not affect any physics under discussion. The results of Y_i^{ee} and N_{ij} (for $i, j = 1, 2, 3$) are listed in the Appendix. Then \tilde{X}_i^{ee} can be explicitly figured out with the help of Eq. (6). As a result, the analytical approximations of \hat{X}_i^{ee} defined below Eq. (8) turn out to be

$$\begin{aligned}
\hat{X}_1^{ee} &\simeq |U_{e1}|^2(1 + 2\beta|U_{e3}|^2) + \frac{1}{2\alpha}(4\beta|U_{e1}|^2|U_{e2}|^2 - \xi_4) - \frac{(|U_{e1}|^2 - |U_{e2}|^2)}{\alpha^2} \left(3\beta^2|U_{e1}|^2|U_{e2}|^2 + \frac{\xi_3}{2} \right) , \\
\hat{X}_2^{ee} &\simeq |U_{e2}|^2(1 + 2\beta|U_{e3}|^2) - \frac{1}{2\alpha}(4\beta|U_{e1}|^2|U_{e2}|^2 - \xi_4) + \frac{(|U_{e1}|^2 - |U_{e2}|^2)}{\alpha^2} \left(3\beta^2|U_{e1}|^2|U_{e2}|^2 + \frac{\xi_3}{2} \right) , \\
\hat{X}_3^{ee} &\simeq |U_{e3}|^2[1 - 2\beta(1 - |U_{e3}|^2)] , \tag{16}
\end{aligned}$$

in which

$$\begin{aligned}
\xi_4 &= 2\kappa_{11}(\beta - \gamma)(1 - 2|U_{e3}|^2) + 4\gamma \text{Re}(\kappa_{21}U_{e3}U_{\mu 3}^* + \kappa_{31}U_{e3}U_{\tau 3}^*) - \xi_1 + |U_{e3}|^2(\xi_1 - 2\xi_2) \\
&= \beta\kappa_{11}(1 - |U_{e3}|^2)^2 + \gamma \left[-\kappa_{11}(1 - |U_{e3}|^2)^2 + \kappa_{22}(|U_{\tau 3}|^2 - |U_{e3}|^2|U_{\mu 3}|^2) + \kappa_{33}(|U_{\mu 3}|^2 \right. \\
&\quad \left. - |U_{e3}|^2|U_{\tau 3}|^2) + 2(1 - |U_{e3}|^2) \text{Re}(\kappa_{21}U_{e3}U_{\mu 3}^* + \kappa_{31}U_{e3}U_{\tau 3}^*) \right. \\
&\quad \left. - 2(1 + |U_{e3}|^2) \text{Re}(\kappa_{32}U_{\mu 3}U_{\tau 3}^*) \right] .
\end{aligned} \tag{17}$$

The explicit expression of $\tilde{P}(\bar{\nu}_e \rightarrow \bar{\nu}_e)$ can therefore be obtained from Eq. (8) with the help of Eq. (16). However, we prefer a different form of $\tilde{P}(\bar{\nu}_e \rightarrow \bar{\nu}_e)$ whose oscillation terms depend on $\tilde{\Delta}_{21}$ and $\tilde{\Delta}_* \equiv \tilde{\Delta}_{31} + \tilde{\Delta}_{32}$ [38], because $\tilde{\Delta}_*$ is sensitive to the neutrino mass ordering in a more transparent way. According to Eqs. (2) and (15), we have

$$\begin{aligned}
\tilde{\Delta}_{21} &\simeq \Delta_{21} + A \cos 2\theta_{12} \cos^2 \theta_{13} + A \left(\frac{A}{2\Delta_{21}} \sin^2 2\theta_{12} \cos^4 \theta_{13} + \xi'_3 \right) , \\
\tilde{\Delta}_* &\simeq \Delta_* + A(1 - 3\sin^2 \theta_{13} - \xi'_1 - 2\xi'_2) ,
\end{aligned} \tag{18}$$

where Δ_{21} and $\Delta_* \equiv \Delta_{31} + \Delta_{32}$ are the counterparts of $\tilde{\Delta}_{21}$ and $\tilde{\Delta}_*$ in vacuum, $\beta \simeq 2\gamma$ has been used, and

$$\begin{aligned}
\xi'_1 &= \frac{1}{2} \left[\kappa_{11}(1 - |U_{e3}|^2) - \kappa_{22}(1 - |U_{\mu 3}|^2) - \kappa_{33}(1 - |U_{\tau 3}|^2) \right. \\
&\quad \left. + 2\text{Re}(\kappa_{21}U_{e3}U_{\mu 3}^* + \kappa_{31}U_{e3}U_{\tau 3}^* + \kappa_{32}U_{\mu 3}U_{\tau 3}^*) \right] , \\
\xi'_2 &= \frac{1}{2} \left[-\kappa_{11}|U_{e3}|^2 + \kappa_{22}|U_{\mu 3}|^2 + \kappa_{33}|U_{\tau 3}|^2 + 2\text{Re}(\kappa_{21}U_{e3}U_{\mu 3}^* + \kappa_{31}U_{e3}U_{\tau 3}^* + \kappa_{32}U_{\mu 3}U_{\tau 3}^*) \right] , \\
\xi'_3 &= \frac{1}{2} \left\{ \kappa_{11}(|U_{e2}|^2 - |U_{e1}|^2) - \kappa_{22}(|U_{\mu 2}|^2 - |U_{\mu 1}|^2) - \kappa_{33}(|U_{\tau 2}|^2 - |U_{\tau 1}|^2) + 2\text{Re}(\kappa_{21}U_{e3}U_{\mu 3}^* \right. \\
&\quad \left. + \kappa_{31}U_{e3}U_{\tau 3}^* + \kappa_{32}U_{\mu 3}U_{\tau 3}^*) - 4\text{Re}[\kappa_{21}(U_{e3}U_{\tau 2} - U_{e2}U_{\tau 3})(U_{\mu 3}^*U_{\tau 2}^* - U_{\mu 2}^*U_{\tau 3}^*) \right. \\
&\quad \left. + \kappa_{31}(U_{e2}U_{\mu 3} - U_{e3}U_{\mu 2})(U_{\mu 3}^*U_{\tau 2}^* - U_{\mu 2}^*U_{\tau 3}^*) + \kappa_{32}(U_{e3}U_{\mu 2} - U_{e2}U_{\mu 3})(U_{e3}^*U_{\tau 2}^* - U_{e2}^*U_{\tau 3}^*) \right\} , \\
\xi'_4 &= \frac{1}{2} \left[\kappa_{11}(1 - |U_{e3}|^2)^2 + \kappa_{22}(|U_{\tau 3}|^2 - |U_{e3}|^2|U_{\mu 3}|^2) + \kappa_{33}(|U_{\mu 3}|^2 - |U_{e3}|^2|U_{\tau 3}|^2) \right. \\
&\quad \left. + 2(1 - |U_{e3}|^2) \text{Re}(\kappa_{21}U_{e3}U_{\mu 3}^* + \kappa_{31}U_{e3}U_{\tau 3}^*) - 2(1 + |U_{e3}|^2) \text{Re}(\kappa_{32}U_{\mu 3}U_{\tau 3}^*) \right] .
\end{aligned} \tag{19}$$

Different from ξ_i (for $i = 1, 2, 3, 4$), ξ'_i are purely the UV parameters. Such a treatment will allow one to see the UV effect in $\tilde{P}(\bar{\nu}_e \rightarrow \bar{\nu}_e)$ more clearly. In Figure 1 we present a numerical illustration of ξ'_i by inputting the 3σ ranges of the neutrino oscillation parameters for the NMO case [46] and choosing the reasonable ranges of the UV parameters (i.e., $\theta_{ij} \lesssim 7.5^\circ$ and $\delta_{ij} \in [0, 2\pi)$ for $i = 1, 2, 3$ and $j = 4, 5, 6$). It is obvious that the magnitudes of ξ'_i are either of the same order as α or much smaller. Since the allowed ranges of $|\xi'_i|$ in the IMO case are very similar to those in the NMO case, they will not necessarily be shown here.

Now let us focus on the probability of $\bar{\nu}_e \rightarrow \bar{\nu}_e$ oscillations. In vacuum we have the elegant expression $P(\bar{\nu}_e \rightarrow \bar{\nu}_e) = 1 - P_0 - P_*$ with [38]

$$\begin{aligned}
P_0 &= \sin^2 2\theta_{12} \cos^4 \theta_{13} \sin^2 F_{21} , \\
P_* &= \frac{1}{2} \sin^2 2\theta_{13} (1 - \cos F_* \cos F_{21} + \cos 2\theta_{12} \sin F_* \sin F_{21}) ,
\end{aligned} \tag{20}$$

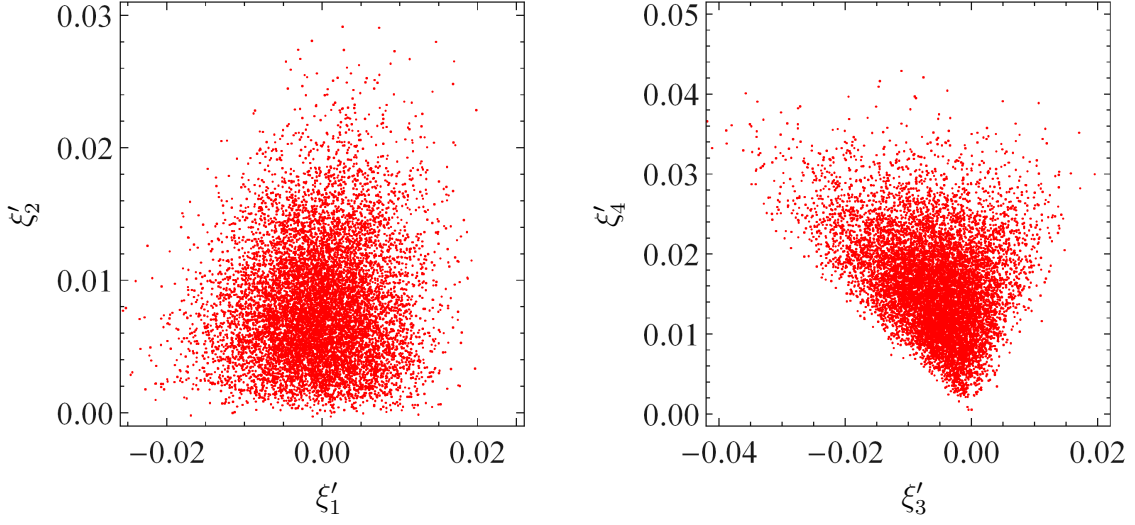


Figure 1: An illustration of ξ'_i given in Eq. (19) by inputting the 3σ ranges of the six neutrino oscillation parameters (i.e., Δ_{21} , Δ_{31} , θ_{12} , θ_{13} , θ_{23} and δ_{13}) for the NMO case [46] and choosing the UV parameters in the ranges $\theta_{ij} \lesssim 7.5^\circ$ and $\delta_{ij} \in [0, 2\pi)$ (for $i = 1, 2, 3$ and $j = 4, 5, 6$).

in which the term proportional to $\sin F_*$ is sensitive to the neutrino mass ordering. In matter with the UV effect, the expression of $\tilde{P}(\bar{\nu}_e \rightarrow \bar{\nu}_e)$ shown in Eq. (8) can analogously be rewritten as $\tilde{P}(\bar{\nu}_e \rightarrow \bar{\nu}_e) = 1 - \tilde{P}_0 - \tilde{P}_*$, where \tilde{P}_0 represents the $\tilde{\Delta}_{21}$ -triggered oscillation and \tilde{P}_* stands for the $\tilde{\Delta}_*$ -triggered oscillation. Taking account of Eqs. (2), (8), (15), (16) and (18), we first define

$$\begin{aligned}\tilde{P}_0 &= P_0 + P_0^{M_1} + P_0^{M_2} + P_0^{\text{UV}}, \\ \tilde{P}_* &= P_* + P_*^{M_1} + P_*^{M_2} + P_*^{\text{UV}},\end{aligned}\tag{21}$$

and then obtain

$$\begin{aligned}P_0^{M_1} &\simeq A \sin^2 2\theta_{12} \cos 2\theta_{12} \cos^6 \theta_{13} \left(1267 \frac{L}{E} \sin 2F_{21} - \frac{2}{\Delta_{21}} \sin^2 F_{21} \right), \\ P_0^{M_2} &\simeq A^2 \sin^2 2\theta_{12} \cos^8 \theta_{13} \left\{ 1267 \frac{L}{E} \left[\frac{1}{2\Delta_{21}} (1 - 5 \cos^2 2\theta_{12}) \sin 2F_{21} \right. \right. \\ &\quad \left. \left. + 1267 \frac{L}{E} \cos^2 2\theta_{12} \cos 2F_{21} \right] - \frac{1}{\Delta_{21}^2} (1 - 4 \cos^2 2\theta_{12}) \sin^2 F_{21} \right\} \\ &\quad + \frac{A}{\Delta_{31}} \sin^2 2\theta_{12} \sin^2 2\theta_{13} \cos^2 \theta_{13} \sin^2 F_{21}, \\ P_0^{\text{UV}} &\simeq A \sin^2 2\theta_{12} \cos^2 \theta_{13} \left[1267 \xi'_3 \frac{L}{E} \cos^2 \theta_{13} \sin 2F_{21} + \frac{2}{\Delta_{21}} (\xi'_3 \cos 2\theta_{12} \cos^2 \theta_{13} \right. \\ &\quad \left. + \xi'_4) \frac{\cos 2\theta_{12}}{\sin^2 2\theta_{12}} \sin^2 F_{21} \right];\end{aligned}\tag{22}$$

and

$$\begin{aligned}
P_*^{M_1} &\simeq \frac{1}{2}A \sin^2 2\theta_{13} \left\{ 1267 \frac{L}{E} \left[(1 + \cos^2 2\theta_{12} \cos^2 \theta_{13} - 3 \sin^2 \theta_{13}) \sin F_* \cos F_{21} \right. \right. \\
&\quad \left. \left. + 2 \cos 2\theta_{12} \cos 2\theta_{13} \cos F_* \sin F_{21} \right] + \frac{1}{\Delta_{21}} \sin^2 2\theta_{12} \cos^2 \theta_{13} \sin F_* \sin F_{21} \right\} , \\
P_*^{M_2} &\simeq \frac{1}{4}A^2 \sin^2 2\theta_{13} \left\{ 1267 \frac{L}{E\Delta_{21}} \sin^2 2\theta_{12} \cos^2 \theta_{13} \left[(3 - 7 \sin^2 \theta_{13}) \cos F_* \sin F_{21} + 3 \cos 2\theta_{12} \right. \right. \\
&\quad \times \cos^2 \theta_{13} \sin F_* \cos F_{21} \left. \right] - \frac{3}{\Delta_{21}^2} \sin^2 2\theta_{12} \cos 2\theta_{12} \cos^4 \theta_{13} \sin F_* \sin F_{21} + \left(1267 \frac{L}{E} \right)^2 \left[\right. \\
&\quad \left. \left[1 + 3 \cos^2 2\theta_{12} - 2 \sin^2 \theta_{13} (3 + 5 \cos^2 2\theta_{12}) + \sin^4 \theta_{13} (9 + 7 \cos^2 2\theta_{12}) \right] \cos F_* \cos F_{21} \right. \\
&\quad \left. - \cos 2\theta_{12} \left[3 + \cos^2 2\theta_{12} - 2 \sin^2 \theta_{13} (7 + \cos^2 2\theta_{12}) + \sin^4 \theta_{13} (15 + \cos^2 2\theta_{12}) \right] \right. \\
&\quad \left. \times \sin F_* \sin F_{21} \right\} - \frac{A}{\Delta_{31}} \cos 2\theta_{13} \sin^2 2\theta_{13} (1 - \cos F_* \cos F_{21} + \cos 2\theta_{12} \sin F_* \sin F_{21}) , \\
P_*^{UV} &\simeq \frac{1}{2}A \sin^2 2\theta_{13} \left\{ 1267 \frac{L}{E} \left[\xi'_3 (\cos F_* \sin F_{21} + \cos 2\theta_{12} \sin F_* \cos F_{21}) - (\xi'_1 + 2\xi'_2) \right. \right. \\
&\quad \times (\cos 2\theta_{12} \cos F_* \sin F_{21} + \sin F_* \cos F_{21}) \left. \right] - \frac{1}{\Delta_{21}} (\xi'_3 \cos 2\theta_{12} \\
&\quad \left. \left. + \frac{1}{\cos^2 \theta_{13}} \xi'_4) \sin F_* \sin F_{21} \right\} . \tag{23}
\end{aligned}$$

One can see that Eqs. (22) and (23) correspond to the matter- and UV-induced corrections to the P_0 and P_* terms, respectively. Considering the smallness of $\sin \theta_{13}$, let us simplify Eq. (23) to some extent as follows:

$$\begin{aligned}
P_*^{M_1} &= \frac{1}{2}A \sin^2 2\theta_{13} \left\{ 1267 \frac{L}{E} \left[(1 + \cos^2 2\theta_{12} \cos^2 \theta_{13} - 3 \sin^2 \theta_{13}) \sin F_* \cos F_{21} \right. \right. \\
&\quad \left. \left. + 2 \cos 2\theta_{12} \cos 2\theta_{13} \cos F_* \sin F_{21} \right] + \frac{1}{\Delta_{21}} \sin^2 2\theta_{12} \cos^2 \theta_{13} \sin F_* \sin F_{21} \right\} , \\
P_*^{M_2} &= \frac{1}{4}A^2 \sin^2 2\theta_{13} \left\{ 1267 \frac{3L}{E\Delta_{21}} \sin^2 2\theta_{12} (\cos F_* \sin F_{21} + \cos 2\theta_{12} \sin F_* \cos F_{21}) \right. \\
&\quad \left. - \frac{3}{\Delta_{21}^2} \sin^2 2\theta_{12} \cos 2\theta_{12} \sin F_* \sin F_{21} + \left(1267 \frac{L}{E} \right)^2 \left[(1 + 3 \cos^2 2\theta_{12}) \cos F_* \cos F_{21} \right. \right. \\
&\quad \left. \left. - \cos 2\theta_{12} (3 + \cos^2 2\theta_{12}) \sin F_* \sin F_{21} \right] \right\} - \frac{A}{\Delta_{31}} \sin^2 2\theta_{13} (1 - \cos F_* \cos F_{21} \\
&\quad + \cos 2\theta_{12} \sin F_* \sin F_{21}) , \\
P_*^{UV} &= \frac{1}{2}A \sin^2 2\theta_{13} \left\{ 1267 \frac{L}{E} \left[\xi'_3 (\cos F_* \sin F_{21} + \cos 2\theta_{12} \sin F_* \cos F_{21}) - (\xi'_1 + 2\xi'_2) \right. \right. \\
&\quad \times (\cos 2\theta_{12} \cos F_* \sin F_{21} + \sin F_* \cos F_{21}) \left. \right] - \frac{1}{\Delta_{21}} (\xi'_3 \cos 2\theta_{12} + \xi'_4) \sin F_* \sin F_{21} \left. \right\} . \tag{24}
\end{aligned}$$

Note that the above analytical approximations are valid for both the NMO and IMO cases, but can only be applied to the antineutrino oscillations. As for the neutrino case, one ought to make the replacement of $\beta \rightarrow -\beta$ and $\gamma \rightarrow -\gamma$. Some discussions are in order.

- In the presence of indirect UV, our main analytical results for $\tilde{P}(\bar{\nu}_e \rightarrow \bar{\nu}_e)$ are summarized in Eqs. (21), (22) and (24). We have done the expansions up to $\mathcal{O}(\alpha^2)$ in our calculations,

in which $A/\Delta_{21} \sim 1267AL/E \sim 10^{-2} \sim \mathcal{O}(\alpha)$ is taken into account. The leading-order oscillation terms $P_0^{M_1}$ and $P_*^{M_1}$ are consistent with those obtained in Ref. [38], where the UV effect was not considered. In contrast, $P_0^{M_2}$, $P_*^{M_2}$, P_0^{UV} and P_*^{UV} appear as the next-to-leading-order oscillation terms of $\tilde{P}(\bar{\nu}_e \rightarrow \bar{\nu}_e)$. Among these four new terms, $P_0^{M_2}$ and $P_*^{M_2}$ describe the fine terrestrial matter effects, and the other two characterize the comparable or much smaller indirect UV effect.

- One can see that the UV effect is always smaller than terrestrial matter effects, and their entanglement does not appear until the next-to-leading-order oscillating terms are taken into account. As for the UV-induced terms, P_0^{UV} is modulated by the Δ_{21} -driven oscillation while P_*^{UV} is the oscillation term related to Δ_* and might therefore affect the determination of the neutrino mass ordering. Since both of them appear as the next-to-leading-order terms as compared with $P_0^{M_1}$ and $P_*^{M_1}$, however, their effects must be strongly suppressed.
- In this paper, we only focus the indirect UV effect in which the masses of sterile neutrinos are larger than the electroweak interaction scale. There is also another type of direct UV effect, where sterile neutrinos can be produced and directly participate in the neutrino propagation process. Different from the indirect UV effect considered here, sterile neutrinos in the direct UV framework will contribute additional terms to the neutrino oscillation probability. In case that the oscillatory behavior can be observed, it will be tested or constrained in the short baseline oscillations [9, 10, 11, 12, 13] for the mass-squared difference at around 1 eV² and at the JUNO-like experiment for the mass-squared difference from 10⁻⁵ eV² to 10⁻¹ eV² [35]. If these additional oscillations are averaged out, it will be similar to the indirect UV effect, but with an additional constant term appeared as shown in Ref. [33, 44]. According to Ref. [45], the limit on the corresponding active-sterile mixing will be relatively weaker in comparison to the indirect UV effect.

3 Numerical simulations

In this section we shall first estimate the orders of magnitude of the oscillation terms associated with the UV and terrestrial matter effects using a JUNO-like detector, and then illustrate whether and how they can affect the neutrino mass ordering determination and precision measurements of Δ_{21} and θ_{12} . In our calculation the best-fit values of six active neutrino oscillation parameters are taken from a global analysis of current three-flavor oscillation experiments [46], with $\Delta_{21} \simeq 7.56 \times 10^{-5}$ eV², $\sin^2 \theta_{12} \simeq 0.321$, $\Delta_* \simeq 5.024 \times 10^{-3}$ eV², $\sin^2 \theta_{13} \simeq 0.022$, $\sin^2 \theta_{23} \simeq 0.430$ and $\delta \simeq 252^\circ$ for the NMO case, and with $\Delta_{21} \simeq 7.56 \times 10^{-5}$ eV², $\sin^2 \theta_{12} \simeq 0.321$, $\Delta_* \simeq -5.056 \times 10^{-3}$ eV², $\sin^2 \theta_{13} \simeq 0.021$, $\sin^2 \theta_{23} \simeq 0.596$ and $\delta \simeq 259^\circ$ for the IMO case. The averaged terrestrial matter density along the reactor antineutrino trajectory is taken as $\rho \simeq 2.6$ g/cm³ [47]. To illustrate the UV effect, we typically take $\theta_{14} = \theta_{24} = \theta_{34} = \theta_{15} = \theta_{25} = \theta_{35} = \theta_{16} = \theta_{26} = \theta_{36} = 5^\circ$, $\delta_{14} = \delta_{15} = \delta_{16} = 120^\circ$, $\delta_{24} = \delta_{25} = \delta_{26} = 60^\circ$ and $\delta_{34} = \delta_{35} = \delta_{36} = 0^\circ$. In addition, for the sensitivity calculation, we assume a JUNO-like 20-kiloton liquid scintillator detector with the energy resolution of 3%/√ E (MeV). The reactor power and baseline distributions are taken from

Tab. 1 of Ref. [48], a total thermal power of 36 GW_{th} and a weighted baseline of 52.5 km. We assume the nominal running time of six years and 300 effective days per year in our numerical simulations. All the statistical and systematical setups are the same as those in Ref. [38], where one can find all the simulation details. The only exception is that here we have enlarged the flux normalization uncertainty to 10% in order to accommodate the reactor antineutrino anomaly and UV-induced zero-distance effect.

In Figure 2 we illustrate the numerical orders of magnitude of the matter-induced and UV-induced corrections to the oscillation probability, where the first and second rows are for the absolute and relative differences of the matter-induced correction respectively, and the third and fourth rows are for the absolute and relative differences of the UV-induced correction respectively. In the left and right panels we show the NMO and IMO cases respectively. For illustration, we define the absolute error induced by the UV and matter effects as

$$\begin{aligned}
\Delta P_{\text{UV}} &= \tilde{P}(\bar{\nu}_e \rightarrow \bar{\nu}_e) - \tilde{P}(\bar{\nu}_e \rightarrow \bar{\nu}_e, \kappa = \mathbf{0}) \\
&\simeq - (P_0^{\text{UV}} + P_*^{\text{UV}}) , \\
\Delta P_{\text{M}} &= \tilde{P}(\bar{\nu}_e \rightarrow \bar{\nu}_e) - \tilde{P}(\bar{\nu}_e \rightarrow \bar{\nu}_e, A = 0) \\
&\simeq - \left(P_0^{\text{M}_1} + P_0^{\text{M}_2} + P_0^{\text{UV}} + P_*^{\text{M}_1} + P_*^{\text{M}_2} + P_*^{\text{UV}} \right) , \tag{25}
\end{aligned}$$

where $\tilde{P}(\bar{\nu}_e \rightarrow \bar{\nu}_e, \kappa = \mathbf{0})$ denotes $\tilde{P}(\bar{\nu}_e \rightarrow \bar{\nu}_e)$ in Eq. (8) by taking $\kappa = \mathbf{0}$ with $\mathbf{0}$ meaning all the elements of κ are zero (i.e., turning off the UV effect), and $\tilde{P}(\bar{\nu}_e \rightarrow \bar{\nu}_e, A = 0)$ stands for $\tilde{P}(\bar{\nu}_e \rightarrow \bar{\nu}_e)$ with $A = 0$ (i.e., back to the case in vacuum). Compared to the left panel of Fig. 1 in Ref. [38], here the absolute difference ΔP_{M} is defined in a generic framework with three active neutrinos and three heavy sterile neutrinos, and it includes the interference terms of the UV and matter potential parameters. The solid and dashed lines are shown for the exact numerical calculation and analytical approximations in Eqs. (21), (22) and (24), respectively. From the first and second rows, we can observe that the absolute and relative orders of magnitude of the matter-induced corrections can reach the levels of 0.6% and 4% respectively, consistent with those in Ref. [38] without the UV effect. On the other hand, the absolute and relative orders of magnitude of the UV-induced corrections are at most 0.02% and 0.1% according to the third and fourth rows. This is because the UV effect is always entangled with matter effects and appears at the next-to-leading order. The same conclusion can be drawn in Figure 3 where the individual terms of the expansion done in Eqs. (21), (22) and (24) are illustrated. The upper panels are for the leading oscillation terms $P_0^{\text{M}_1}$ and $P_*^{\text{M}_1}$, and the four next-to-leading terms are illustrated in the lower panels. The left and right panels are shown for the NMO and IMO cases respectively. To show how the UV-induced corrections depend on the standard oscillation and UV parameters, we illustrate the scattering plots of the UV-induced corrections in Figure 4 by varying the six oscillation parameters ($\Delta_{21}, \Delta_{31}, \theta_{12}, \theta_{13}, \theta_{23}, \delta_{13}$) within their 3σ ranges for the NMO case, and the UV parameters θ_{ij} ($i = 1, 2, 3, j = 4, 5, 6$) and δ_{ij} ($i = 1, 2, 3, j = 4, 5, 6$) in the ranges of $[0, 7.5^\circ]$ and $[0, 360^\circ]$ respectively. The left and right panels are shown for the exact numerical calculation and analytical approximations respectively. We conclude that the absolute magnitudes of the UV-induced corrections are within the region of smaller than 0.05%.

In Figure 5 we illustrate the terrestrial matter (left panel) and UV (right panel) effects on the

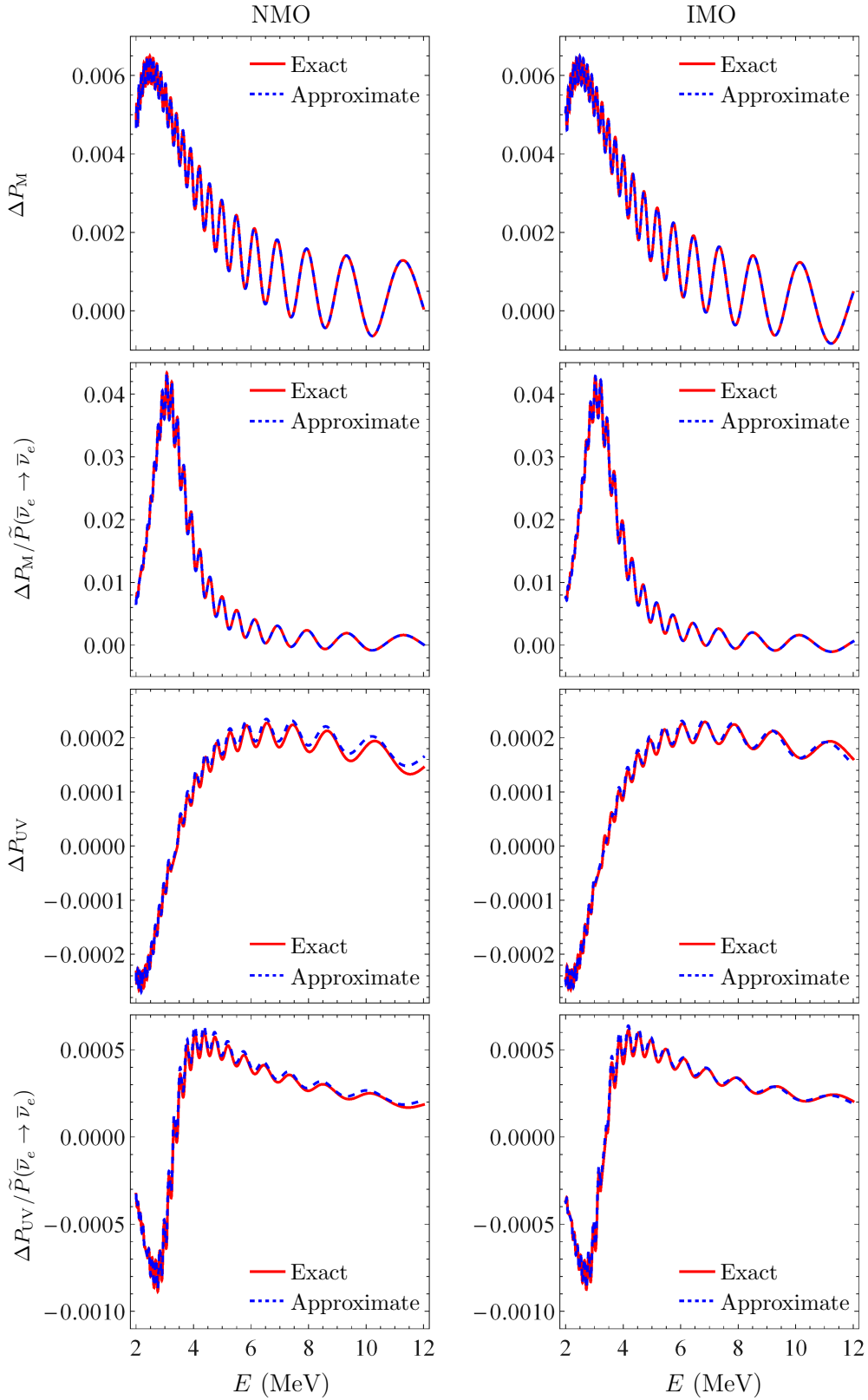


Figure 2: Numerical orders of magnitude of the matter-induced and UV-induced corrections to the oscillation probability, where the first (third) and second (fourth) rows are for the absolute and relative differences of the matter-induced (UV-induced) correction respectively. The left and right panels are shown for the NMO and IMO cases respectively. The solid and dashed lines are shown for the exact numerical calculations and analytical approximations respectively.

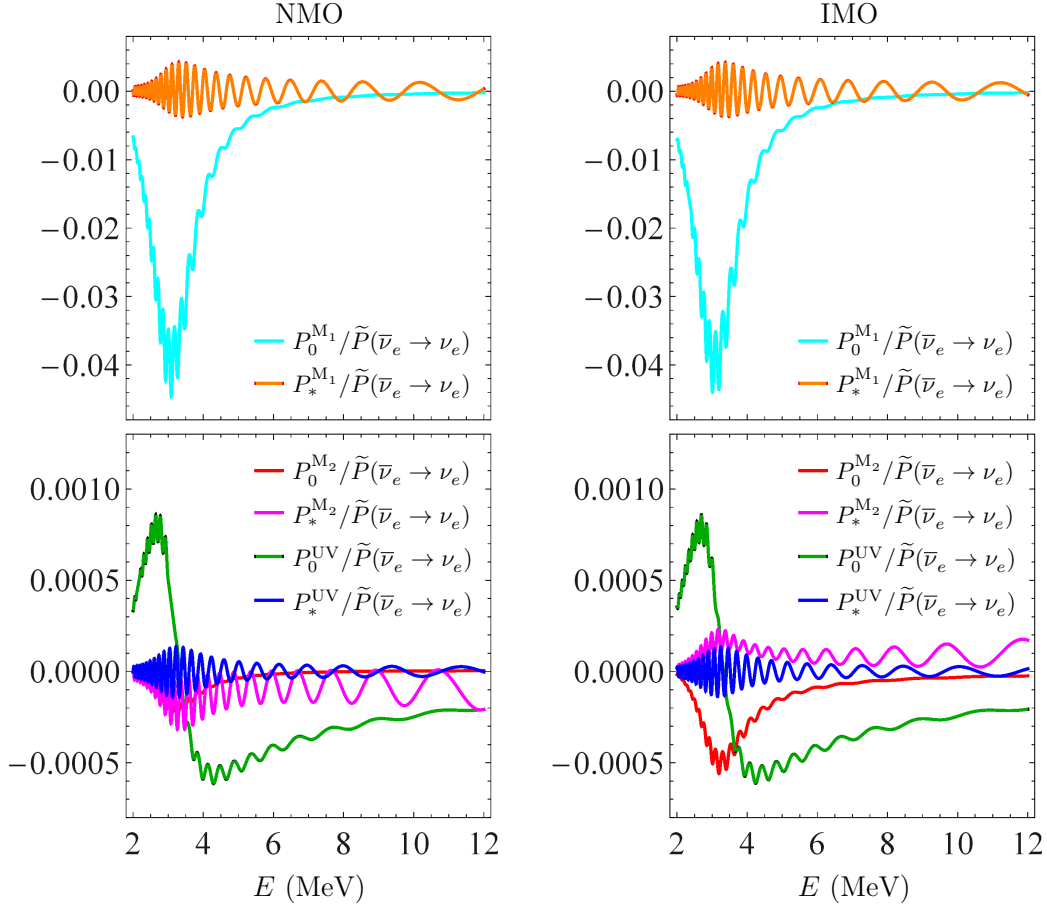


Figure 3: The relative numerical orders of magnitude of the individual expansion terms in Eqs. (22) and (24) to the analytical approximations of $\tilde{P}(\bar{\nu}_e \rightarrow \bar{\nu}_e)$. The upper panels are for the leading oscillation terms $P_0^{M_1}$ and $P_*^{M_1}$, and the four next-to-leading terms are illustrated in the lower panels. The left and right panels are shown for the NMO and IMO cases respectively.

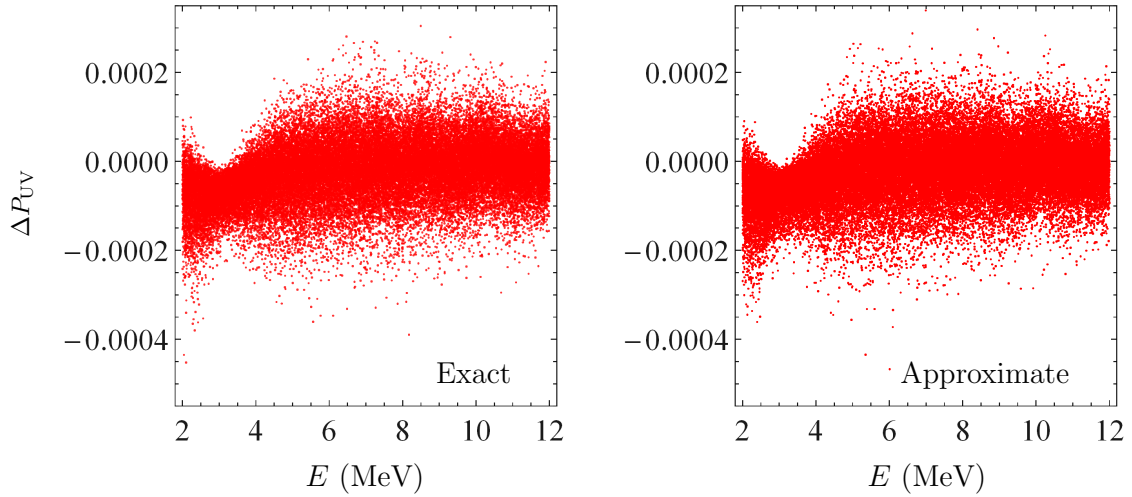


Figure 4: Scattering plots of the UV-induced corrections by varying the six oscillation parameters (Δ_{21} , Δ_{31} , θ_{12} , θ_{13} , θ_{23} , δ_{13}) within their 3σ ranges for the NMO case, and the UV parameters θ_{ij} ($i = 1, 2, 3$, $j = 4, 5, 6$) and δ_{ij} ($i = 1, 2, 3$, $j = 4, 5, 6$) in the ranges of $[0, 7.5^\circ]$ and $[0, 360^\circ]$ respectively. The left and right panels are shown for the exact numerical calculations and analytical approximations respectively.

neutrino mass ordering sensitivity in the generic framework of three active neutrinos and three heavy sterile neutrinos. In each panel the vertical distances of the black and red lines are defined as the sensitivity of the mass ordering (i.e., $\Delta\chi^2 = |\chi_{\min}^2(\text{NMO}) - \chi_{\min}^2(\text{IMO})|$, where the least squares function χ^2 is defined as in Eq. (20) of Ref. [38] and χ_{\min}^2 is the minimum of χ^2 after the marginalization of all the oscillation and pull parameters). The solid lines are for the case considering both the matter and UV effects and the dashed lines are the scenario of neglecting the matter effects (left panel) or neglecting the UV effect (right panel). Note that the red dashed line in the right panel has been horizontally shifted by $-0.35 \times 10^{-5} \text{ eV}^2$ to avoid the overlap of the curves. In the left panel, the inclusion of terrestrial matter effects can reduce $\Delta\chi^2$ by 0.61 from 9.89 to 9.28. This conclusion is consistent with that in Ref. [38] for the three neutrino mixing case ($\Delta\chi^2$ reduced by 0.64 from 10.28 to 9.64). The absolute value of $\Delta\chi^2$ is reduced mainly because the true three neutrino oscillation parameters have been changed to those in Ref. [46]. The size of $\Delta\chi^2$ reduction by 0.61 is non-negligible because it can be comparable with other systematic uncertainties. On the other hand, one can observe from the right panel that the inclusion of the UV effect only change $\Delta\chi^2$ from 9.31 to 9.28, resulting in a reduction of $\Delta\chi^2 \simeq 0.03$, which is much smaller than that of terrestrial matter effects. By randomly sampling the UV parameters θ_{ij} ($i = 1, 2, 3, j = 4, 5, 6$) and δ_{ij} ($i = 1, 2, 3, j = 4, 5, 6$) in the ranges of $[0, 7.5^\circ]$ and $[0, 360^\circ]$ respectively, we find that the variation of $\Delta\chi^2$ is well within the ± 0.04 range around 9.28, which demonstrates the robustness of the mass ordering measurement against the possible UV effect in the JUNO experiment.

Next we are going to discuss the UV and terrestrial matter effects in the precision measurement of θ_{12} and Δ_{21} . In Figure 6 we illustrate the fitting results of θ_{12} and Δ_{21} where both the matter and UV effects are included in the measured neutrino spectrum but the matter effects (left panel) or the UV corrections (right panel) are neglected in the predicted neutrino spectrum. The red stars and blue circles are the true values and best-fit values of θ_{12} and Δ_{21} , respectively. From the left panel for the case of neglecting matter effects, one can observe that the best-fit values of θ_{12} and Δ_{21} deviate around 2.0σ and 0.7σ from their true values, with the parameter precisions of 0.63% and 0.29% respectively. The levels of deviations for the fitted θ_{12} and Δ_{21} are similar to those obtained in Ref. [38] where the three-flavor oscillation framework is considered. Thus terrestrial matter effects are of importance for future precision spectral measurements of reactor antineutrino oscillations. Regarding the case of neglecting the UV effect as shown in the right panel, the deviations of the best-fit values for θ_{12} and Δ_{21} are within the size of 0.1σ with the parameter precisions of 0.60% and 0.27% respectively. The parameter accuracies in the left panel are a little bit worse because additional marginalization has been performed for the UV parameters in the same regions as in Figure 4. Therefore the precision measurement of θ_{12} and Δ_{21} in the generic framework of three active neutrinos and three heavy sterile neutrinos turns out to be rather robust for the reasonable UV parameter space.

Before finishing this section, we want to remark on the indirect UV effect in the accelerator neutrino experiments. Different from the oscillation channel $\bar{\nu}_e \rightarrow \bar{\nu}_e$ for the reactor antineutrino experiments discussed here, the indirect UV effect in long baseline accelerator neutrino experiments may be significant because the terrestrial matter effect becomes larger and its entanglement with the indirect UV effect will also be non-negligible. The additional mixing angles and CP-violating

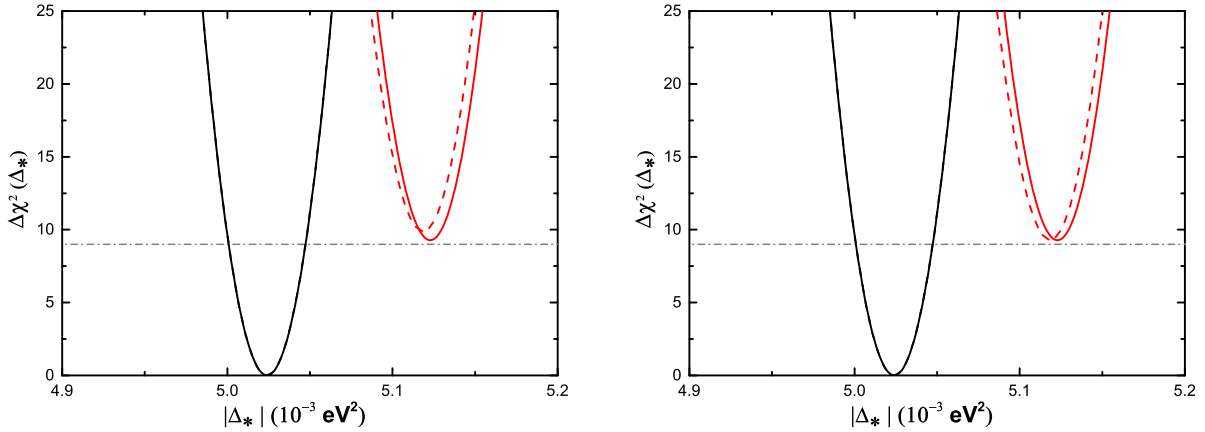


Figure 5: Terrestrial matter (left panel) and UV (right panel) effects on the neutrino mass ordering sensitivity in the generic framework of three active neutrinos and three heavy sterile neutrinos. The solid lines are for the case considering both matter and UV effects, where the black and red ones come from the fitting assuming the NMO and IMO cases of three active neutrinos, respectively. The dashed lines are the scenario of neglecting the matter effects (left panel) or neglecting the UV effect (right panel). In each panel the vertical distances between the minima of the black and red lines are defined as the sensitivity of the mass ordering (i.e., $\Delta\chi^2$).

phases will induce multiple parameter degeneracy problem and the sensitivities to the neutrino mass ordering, leptonic CP violation and the θ_{23} octant will be largely affected [23, 24, 25, 26, 27, 28, 29, 30]. Taking the DUNE experiment as an example, the discovery potential for maximal CP violation would be degraded from 6σ to the 3.7σ for seven years of nominal running if the indirect UV effect is considered [30]. A robust method to remove the parameter degeneracy and have better sensitivities to the three neutrino oscillation and new physics effects would be the combinations of accelerator neutrino experiments with different baselines, different neutrino energies and different neutrino oscillation channels [30].

4 Summary

We have examined whether the JUNO-like reactor antineutrino oscillation experiment can be used to probe the indirect UV effect caused by small corrections of heavy sterile neutrinos to the 3×3 PMNS matrix. In this regard we have paid particular attention to how such an effect is entangled with terrestrial matter effects in $\bar{\nu}_e \rightarrow \bar{\nu}_e$ oscillations. After deriving the oscillation probability in a good analytical approximation for the antineutrino beam energy of a few MeV, we have done some numerical simulations based on the setup of a 20-kiloton JUNO-like liquid scintillator detector. We find that the indirect UV effect is always smaller than terrestrial matter effects, and their entanglement does not appear until the next-to-leading-order oscillating terms are taken into account. Two immediate conclusions turn out to be: (a) indirect UV makes no difference in the JUNO-like experiment; and (b) such an experiment's sensitivities to the neutrino mass ordering and a precision measurement of θ_{12} and Δ_{21} are robust.

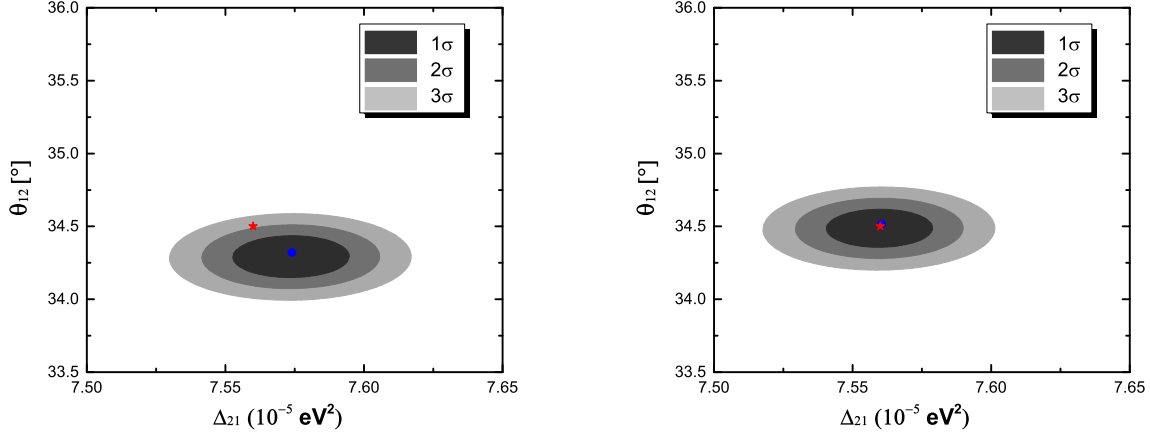


Figure 6: Allowed regions of θ_{12} and Δ_{21} by neglecting the terrestrial matter (left panel) or UV (right panel) effects in the predictions. Both effects are included in the measurements. The red stars and blue circles are the true values and best-fit values of θ_{12} and Δ_{21} , respectively.

Although the indirect UV effect is too small to be accessible in the JUNO-like reactor-based antineutrino oscillation experiment, it may be probed or constrained in some accelerator-based long-baseline neutrino oscillation experiments. In either case terrestrial matter effects should be carefully studied, so as to make them distinguishable from the fundamental new physics effects.

Acknowledgments

One of us (ZZX) would like to thank H. Päs for his warm hospitality and useful discussions at the Technische Universität Dortmund, where this paper was finalized. This work was supported in part by the National Natural Science Foundation of China under Grant No. 11305193 (YFL) and Grant No. 11775231 (ZZX and JYZ).

Appendix

One may calculate $Y_k^{ee} = (V^* \tilde{\mathcal{H}}^{k-1} V^T)^{ee}$ and N_{jk} (for $j, k = 1, 2, 3$) in Eqs. (6) and (7) with the replacements $\tilde{\mathcal{H}} \rightarrow \tilde{\mathcal{H}}' = \tilde{\mathcal{H}} - E_1 \mathbf{1}$, and $\tilde{E}_i \rightarrow \tilde{E}'_i = \tilde{E}_i - E_1 = \lambda_i \Delta_{31} / (2E)$. The explicit expressions of Y_i^{ee} in our approximations are

$$\begin{aligned}
Y_1^{ee} &\simeq \left(1 - \frac{\kappa_{11}}{2}\right)^2, \\
Y_2^{ee} &\simeq \frac{\Delta_{31}}{2E} \left(1 - \frac{\kappa_{11}}{2}\right)^2 \left[|U_{e3}|^2 + |U_{e2}|^2 \alpha - (\beta - \gamma) \left(1 - \frac{\kappa_{11}}{2}\right)^2 + \gamma (|\kappa_{21}|^2 + |\kappa_{31}|^2) \right], \\
Y_3^{ee} &\simeq \frac{\Delta_{31}^2}{4E^2} \left(1 - \frac{\kappa_{11}}{2}\right)^2 \left\{ \left[|U_{e3}|^2 + |U_{e2}|^2 \alpha - (\beta - \gamma) \left(1 - \frac{\kappa_{11}}{2}\right)^2 + \gamma (|\kappa_{21}|^2 + |\kappa_{31}|^2) \right]^2 \right. \\
&\quad \left. + \left| U_{e3}^* U_{\mu 3} + \alpha U_{e2}^* U_{\mu 2} - \gamma \left[\kappa_{21} \left(1 - \frac{\kappa_{22}}{2}\right) - \kappa_{31} \kappa_{32}^* \right] \right|^2 \right. \\
&\quad \left. + \left| U_{e3}^* U_{\tau 3} + \alpha U_{e2}^* U_{\tau 2} - \gamma \kappa_{31} \left(1 - \frac{\kappa_{33}}{2}\right) \right|^2 \right\}, \tag{26}
\end{aligned}$$

where each Y_i^{ee} has a factor $(1 - \kappa_{11}/2)^2$. Moreover, we obtain

$$\begin{aligned}
N_{11} &\simeq 1 + \frac{1}{\alpha} \left[(1 + \alpha) (\gamma - \beta |U_{e1}|^2) + \frac{\xi_1}{2} \right] + \frac{1}{\alpha^2} [\beta^2 |U_{e1}|^2 (|U_{e1}|^2 - 2|U_{e2}|^2) \\
&\quad - \beta \gamma (|U_{e1}|^2 - |U_{e2}|^2) - \frac{\xi_3}{2}] , \\
N_{21} &\simeq -\frac{1}{\alpha} \left[(1 + \alpha) (\gamma - \beta |U_{e1}|^2) + \frac{\xi_1}{2} \right] - \frac{1}{\alpha^2} [\beta^2 |U_{e1}|^2 (|U_{e1}|^2 - 2|U_{e2}|^2) \\
&\quad - \beta \gamma (|U_{e1}|^2 - |U_{e2}|^2) - \frac{\xi_3}{2}] , \\
N_{31} &\simeq 0 ;
\end{aligned} \tag{27}$$

$$\begin{aligned}
N_{12} &\simeq \frac{2E}{\Delta_{31}} \left\{ -1 + \beta (|U_{e1}|^2 - |U_{e3}|^2) - \frac{1}{\alpha} [1 + 2(\gamma - \beta |U_{e1}|^2) + \xi_1] + \frac{1}{\alpha^2} [\beta (1 + 2\gamma) (|U_{e1}|^2 \right. \\
&\quad - |U_{e2}|^2) - 2\beta^2 |U_{e1}|^2 (|U_{e1}|^2 - 2|U_{e2}|^2) + \xi_3] - \frac{1}{\alpha^3} [\beta^2 (|U_{e1}|^4 - 4|U_{e1}|^2 |U_{e2}|^2 + |U_{e2}|^4) \\
&\quad \left. - \xi_3] + \frac{\beta (|U_{e1}|^2 - |U_{e2}|^2)}{\alpha^4} [\beta^2 (|U_{e1}|^4 - 6|U_{e1}|^2 |U_{e2}|^2 + |U_{e2}|^4) - 2\xi_3] \right\} , \\
N_{22} &\simeq \frac{2E}{\Delta_{31}} \left\{ 1 - \beta (1 + |U_{e1}|^2 - 2|U_{e3}|^2) + 2\gamma + \alpha + \alpha^2 + \frac{1}{\alpha} [1 + 2(\gamma - \beta |U_{e1}|^2) + \xi_1] \right. \\
&\quad - \frac{1}{\alpha^2} [\beta (1 + 2\gamma) (|U_{e1}|^2 - |U_{e2}|^2) - 2\beta^2 |U_{e1}|^2 (|U_{e1}|^2 - 2|U_{e2}|^2) + \xi_3] \\
&\quad + \frac{1}{\alpha^3} [\beta^2 (|U_{e1}|^4 + |U_{e2}|^4 - 4|U_{e1}|^2 |U_{e2}|^2) - \xi_3] - \frac{\beta (|U_{e1}|^2 - |U_{e2}|^2)}{\alpha^4} [\beta^2 (|U_{e1}|^4 \\
&\quad \left. - 6|U_{e1}|^2 |U_{e2}|^2 + |U_{e2}|^4) - 2\xi_3] \right\} , \\
N_{32} &\simeq -\frac{2E}{\Delta_{31}} [\alpha + \alpha^2 - \beta (1 - |U_{e3}|^2) + 2\gamma] ;
\end{aligned} \tag{28}$$

and

$$\begin{aligned}
N_{13} &\simeq \frac{4E^2}{\Delta_{31}^2} \left\{ \frac{1}{\alpha} \left[1 - \beta (|U_{e1}|^2 - |U_{e3}|^2) + \frac{\xi_1}{2} + \xi_2 \right] - \frac{1}{\alpha^2} [\beta (|U_{e1}|^2 - |U_{e2}|^2) - \beta^2 (|U_{e1}|^4 \right. \\
&\quad - 2|U_{e1}|^2 |U_{e2}|^2 - |U_{e1}|^2 |U_{e3}|^2 + |U_{e2}|^2 |U_{e3}|^2) + \frac{\xi_3}{2}] + \frac{1}{\alpha^3} [\beta^2 (|U_{e1}|^4 - 4|U_{e1}|^2 |U_{e2}|^2 \\
&\quad \left. + |U_{e2}|^4) - \xi_3] - \frac{\beta (|U_{e1}|^2 - |U_{e2}|^2)}{\alpha^4} [\beta^2 (|U_{e1}|^4 - 6|U_{e1}|^2 |U_{e2}|^2 + |U_{e2}|^4) - 2\xi_3] \right\} , \\
N_{23} &\simeq \frac{4E^2}{\Delta_{31}^2} \left\{ -1 - \alpha (1 + \alpha) + \beta (1 - 3|U_{e3}|^2) - \frac{1}{\alpha} \left[1 - \beta (|U_{e1}|^2 - |U_{e3}|^2) + \frac{\xi_1}{2} + \xi_2 \right] \right. \\
&\quad + \frac{1}{\alpha^2} \left[\beta (|U_{e1}|^2 - |U_{e2}|^2) - \beta^2 (|U_{e1}|^4 - 2|U_{e1}|^2 |U_{e2}|^2 - |U_{e1}|^2 |U_{e3}|^2 + |U_{e2}|^2 |U_{e3}|^2) + \frac{\xi_3}{2} \right] \\
&\quad - \frac{1}{\alpha^3} [\beta^2 (|U_{e1}|^4 - 4|U_{e1}|^2 |U_{e2}|^2 + |U_{e2}|^4) - \xi_3] + \frac{\beta (|U_{e1}|^2 - |U_{e2}|^2)}{\alpha^4} [\beta^2 (|U_{e1}|^4 \\
&\quad \left. - 6|U_{e1}|^2 |U_{e2}|^2 + |U_{e2}|^4) - 2\xi_3] \right\} , \\
N_{33} &\simeq \frac{4E^2}{\Delta_{31}^2} [1 + \alpha + \alpha^2 - \beta (1 - 3|U_{e3}|^2)] .
\end{aligned} \tag{29}$$

It is clear that $N_{11} + N_{21} + N_{31} = 1$, $N_{12} + N_{22} + N_{32} = 0$ and $N_{13} + N_{23} + N_{33} = 0$ hold. These three relations are exactly valid, as one can see from Eq. (7).

References

- [1] H. Fritzsch, M. Gell-Mann and P. Minkowski, Vector - Like Weak Currents and New Elementary Fermions, *Phys. Lett.* **59B** (1975) 256.
- [2] P. Minkowski, $\mu \rightarrow e\gamma$ at a Rate of One Out of 10^9 Muon Decays?, *Phys. Lett.* **67B** (1977) 421.
- [3] T. Yanagida, in Proceedings of the Workshop on Unified Theory and the Baryon Number of the Universe, edited by O. Sawada and A. Sugamoto (KEK, Tsukuba, 1979), p. 95.
- [4] M. Gell-Mann, P. Ramond, and R. Slansky, in Supergravity, edited by P. Van Nieuwenhuizen and D. Freedman (North Holland, Amsterdam, 1979), p. 315.
- [5] S.L. Glashow, in Quarks and Leptons, edited by M. Levy, J. L. Basdevant, D. Speiser, J. Weyers, R. Gastmans and M. Jacob (Plenum, New York, 1980), p. 707.
- [6] R. N. Mohapatra and G. Senjanovic, Neutrino Mass and Spontaneous Parity Violation, *Phys. Rev. Lett.* **44** (1980) 912.
- [7] J. Schechter and J. W. F. Valle, Neutrino Masses in SU(2) x U(1) Theories, *Phys. Rev. D* **22** (1980) 2227.
- [8] M. Fukugita and T. Yanagida, Baryogenesis Without Grand Unification, *Phys. Lett. B* **174** (1986) 45.
- [9] K. N. Abazajian *et al.*, Light Sterile Neutrinos: A White Paper, arXiv:1204.5379 [hep-ph].
- [10] S. Gariazzo, C. Giunti, M. Laveder, Y. F. Li and E. M. Zavanin, Light sterile neutrinos, *J. Phys. G* **43**, 033001 (2016) [arXiv:1507.08204 [hep-ph]].
- [11] S. Gariazzo, C. Giunti, M. Laveder and Y. F. Li, Updated Global 3+1 Analysis of Short-BaseLine Neutrino Oscillations, *JHEP* **1706**, 135 (2017) [arXiv:1703.00860 [hep-ph]].
- [12] M. Dentler, Á. Hernández-Cabezudo, J. Kopp, M. Maltoni and T. Schwetz, Sterile neutrinos or flux uncertainties? Status of the reactor anti-neutrino anomaly, *JHEP* **1711** (2017) 099 [arXiv:1709.04294 [hep-ph]].
- [13] C. S. Fong, H. Minakata and H. Nunokawa, Non-unitary evolution of neutrinos in matter and the leptonic unitarity test, arXiv:1712.02798 [hep-ph].
- [14] B. Pontecorvo, Mesonium and anti-mesonium, *Sov. Phys. JETP* **6** (1957) 429 [*Zh. Eksp. Teor. Fiz.* **33** (1957) 549].

- [15] Z. Maki, M. Nakagawa and S. Sakata, Remarks on the unified model of elementary particles, Prog. Theor. Phys. **28** (1962) 870.
- [16] Z. z. Xing, Correlation between the Charged Current Interactions of Light and Heavy Majorana Neutrinos, Phys. Lett. B **660** (2008) 515 [arXiv:0709.2220 [hep-ph]].
- [17] Z. z. Xing, Casas-Ibarra Parametrization and Unflavored Leptogenesis, Chin. Phys. C **34** (2010) 1 [arXiv:0902.2469 [hep-ph]].
- [18] Z. z. Xing, A full parametrization of the 6 X 6 flavor mixing matrix in the presence of three light or heavy sterile neutrinos, Phys. Rev. D **85** (2012) 013008 [arXiv:1110.0083 [hep-ph]].
- [19] S. Antusch, C. Biggio, E. Fernandez-Martinez, M. B. Gavela and J. Lopez-Pavon, Unitarity of the Leptonic Mixing Matrix, JHEP **0610** (2006) 084 [hep-ph/0607020].
- [20] S. Antusch and O. Fischer, Non-unitarity of the leptonic mixing matrix: Present bounds and future sensitivities, JHEP **1410** (2014) 094 [arXiv:1407.6607 [hep-ph]].
- [21] E. Fernandez-Martinez, J. Hernandez-Garcia and J. Lopez-Pavon, Global constraints on heavy neutrino mixing, JHEP **1608** (2016) 033 [arXiv:1605.08774 [hep-ph]].
- [22] M. Blennow, P. Coloma, E. Fernandez-Martinez, J. Hernandez-Garcia and J. Lopez-Pavon, Non-Unitarity, sterile neutrinos, and Non-Standard neutrino Interactions, JHEP **1704** (2017) 153 [arXiv:1609.08637 [hep-ph]].
- [23] S. Antusch, M. Blennow, E. Fernandez-Martinez and J. Lopez-Pavon, Probing non-unitary mixing and CP-violation at a Neutrino Factory, Phys. Rev. D **80** (2009) 033002 [arXiv:0903.3986 [hep-ph]].
- [24] F. J. Escrihuela, D. V. Forero, O. G. Miranda, M. Tortola and J. W. F. Valle, On the description of nonunitary neutrino mixing, Phys. Rev. D **92** (2015) no.5, 053009 Erratum: [Phys. Rev. D **93** (2016) no.11, 119905] [arXiv:1503.08879 [hep-ph]].
- [25] B. Bekman, J. Gluza, J. Holeczek, J. Syska and M. Zralek, Matter effects and CP violating neutrino oscillations with nondecoupling heavy neutrinos, Phys. Rev. D **66** (2002) 093004 [hep-ph/0207015].
- [26] S. F. Ge, P. Pasquini, M. Tortola and J. W. F. Valle, Measuring the leptonic CP phase in neutrino oscillations with nonunitary mixing, Phys. Rev. D **95** (2017) no.3, 033005 [arXiv:1605.01670 [hep-ph]].
- [27] O. G. Miranda, M. Tortola and J. W. F. Valle, New ambiguity in probing CP violation in neutrino oscillations, Phys. Rev. Lett. **117** (2016) no.6, 061804 [arXiv:1604.05690 [hep-ph]].
- [28] F. J. Escrihuela, D. V. Forero, O. G. Miranda, M. Trtola and J. W. F. Valle, Probing CP violation with non-unitary mixing in long-baseline neutrino oscillation experiments: DUNE as a case study, New J. Phys. **19** (2017) no.9, 093005 [arXiv:1612.07377 [hep-ph]].

- [29] S. C and R. Mohanta, Non-unitarity lepton mixing in an inverse seesaw and its impact on the physics potential of long-baseline experiments, arXiv:1708.05372 [hep-ph].
- [30] J. Tang, Y. Zhang and Y. F. Li, Probing Direct and Indirect Unitarity Violation in Future Accelerator Neutrino Facilities, Phys. Lett. B **774** (2017) 217 [arXiv:1708.04909 [hep-ph]].
- [31] Z. z. Xing, Towards testing the unitarity of the 3X3 lepton flavor mixing matrix in a precision reactor antineutrino oscillation experiment, Phys. Lett. B **718** (2013) 1447 [arXiv:1210.1523 [hep-ph]].
- [32] X. Qian, C. Zhang, M. Diwan and P. Vogel, “Unitarity Tests of the Neutrino Mixing Matrix, arXiv:1308.5700 [hep-ex].
- [33] C. S. Fong, H. Minakata and H. Nunokawa, A framework for testing leptonic unitarity by neutrino oscillation experiments, JHEP **1702** (2017) 114 [arXiv:1609.08623 [hep-ph]].
- [34] P. Langacker and D. London, Lepton Number Violation and Massless Nonorthogonal Neutrinos, Phys. Rev. D **38** (1988) 907.
- [35] F. An *et al.* [JUNO Collaboration], Neutrino Physics with JUNO, J. Phys. G **43** (2016) 030401 [arXiv:1507.05613 [physics.ins-det]].
- [36] F. Capozzi, E. Lisi and A. Marrone, Neutrino mass hierarchy and electron neutrino oscillation parameters with one hundred thousand reactor events, Phys. Rev. D **89** (2014) no.1, 013001 [arXiv:1309.1638 [hep-ph]].
- [37] F. Capozzi, E. Lisi and A. Marrone, Neutrino mass hierarchy and precision physics with medium-baseline reactors: Impact of energy-scale and flux-shape uncertainties, Phys. Rev. D **92** (2015) no.9, 093011 [arXiv:1508.01392 [hep-ph]].
- [38] Y. F. Li, Y. Wang and Z. z. Xing, Terrestrial matter effects on reactor antineutrino oscillations at JUNO or RENO-50: how small is small?, Chin. Phys. C **40** (2016) no.9, 091001 [arXiv:1605.00900 [hep-ph]].
- [39] Z. z. Xing and J. y. Zhu, Analytical approximations for matter effects on CP violation in the accelerator-based neutrino oscillations with $E \lesssim 1$ GeV, JHEP **1607** (2016) 011 [arXiv:1603.02002 [hep-ph]].
- [40] Y. F. Li, J. Zhang, S. Zhou and J. y. Zhu, Looking into Analytical Approximations for Three-flavor Neutrino Oscillation Probabilities in Matter, JHEP **1612** (2016) 109 [arXiv:1610.04133 [hep-ph]].
- [41] K. Kimura, A. Takamura and H. Yokomakura, Exact formulas and simple CP dependence of neutrino oscillation probabilities in matter with constant density, Phys. Rev. D **66** (2002) 073005 [hep-ph/0205295].
- [42] O. Yasuda, On the exact formula for neutrino oscillation probability by Kimura, Takamura and Yokomakura, arXiv:0704.1531 [hep-ph].

- [43] E. Fernandez-Martinez, M. B. Gavela, J. Lopez-Pavon and O. Yasuda, CP-violation from non-unitary leptonic mixing, *Phys. Lett. B* **649** (2007) 427 [hep-ph/0703098].
- [44] Y. F. Li and S. Luo, Neutrino Oscillation Probabilities in Matter with Direct and Indirect Unitarity Violation in the Lepton Mixing Matrix, *Phys. Rev. D* **93** (2016) no.3, 033008 [arXiv:1508.00052 [hep-ph]].
- [45] S. Parke and M. Ross-Lonergan, *Phys. Rev. D* **93**, no. 11, 113009 (2016) [arXiv:1508.05095 [hep-ph]].
- [46] P. F. de Salas, D. V. Forero, C. A. Ternes, M. Tortola and J. W. F. Valle, Status of neutrino oscillations 2017, arXiv:1708.01186 [hep-ph].
- [47] I. Mocioiu and R. Shrock, Matter effects on neutrino oscillations in long baseline experiments, *Phys. Rev. D* **62** (2000) 053017 [hep-ph/0002149].
- [48] Y. F. Li, J. Cao, Y. Wang and L. Zhan, Unambiguous Determination of the Neutrino Mass Hierarchy Using Reactor Neutrinos, *Phys. Rev. D* **88**, 013008 (2013), [arXiv:1303.6733 [hep-ex]].